

Equations for filling factor estimation in opal matrix. Addendum to “Deep level emission of ZnO nanoparticles deposited inside UV opal”, [Opt. Commun. 259 (1) (2006) 378–384]

S.M. Abrarov^{a,*}, T.W. Kim^b, T.W. Kang^a

^a Quantum-functional Semiconductor Research Center, Department of Physics, Dongguk University, Seoul 100-715, South Korea

^b Advanced Semiconductor Research Center, Division of Electrical and Computer Engineering, Hanyang University, Seoul 133-791, South Korea

Received 21 December 2005; received in revised form 9 May 2006; accepted 16 May 2006

Abstract

We consider two equations for the filling factor estimation of infiltrated zinc oxide (ZnO) in silica (SiO₂) opal and gallium nitride (GaN) in ZnO opal. The first equation is based on the effective medium approximation, while the second one—on Maxwell–Garnett approximation. The comparison between two filling factors shows that both equations can be equally used for the estimation of the quantity of infiltrated nanoparticles inside opal photonic crystal.

PACS: 42.70.Qs; 78.67.Pt

Keywords: Filling factor; Photonic band-gap; Bragg reflection; Effective refractive index

1. Introduction

Photonic crystals (PhCs) with forbidden band-gaps, proposed by Eli Yablonovitch [1] and Sajeev John [2], open new opportunities for their applications in modern optics. PhCs are one-, two-, and three-dimensional dielectric lattices with periodicity on the order of the optical wavelengths. The implementations of PhCs are mostly aimed to improve the useful properties of various materials as well as opto-electronic devices such as light emitting diodes [3], laser diodes [4], optical fibers [5]. Nowadays research on PhCs becomes an increasingly important in the fundamental and applied sciences.

One of the kinds of PhCs is an opal matrix consisting of spherical sub-micron balls packed into face centered cubic (FCC) structure by means of self-sedimentation in a fluid

suspension [6,7]. Silicon dioxide (SiO₂) or silica is frequently used as a host material in artificial opals. Silica balls are synthesized by Stöber–Fink–Bohn process through the hydrolysis of tetraethylorthosilicate in the ethanol solution mixed with ammonium hydroxide and water [8].

The applications of opal PhCs have number of significant advantages over others. For instance, the opal matrix can be grown over a large practically unlimited plane area. Their fabrication is very technological without requirement for expensive equipment. It has been recently shown that by means of electro-deposition the high quality two- and three-dimensional porous films, patterned in inverted opal, can be successfully realized [9]. Thus, the nanocrystals grown in artificial opal can be regarded as inexpensive and efficient alternative for electro- and photolithography.

The fabrication of the high quality artificial opal by natural self-sedimentation in monodispersed fluid suspension may continue for a long period, up to 10 months [6]. However this drawback is resolved in electrophoretically assisted sedimentation involving an external electric field. Such an original technology enables one to accelerate a

DOI of original article: [10.1016/j.optcom.2005.08.048](https://doi.org/10.1016/j.optcom.2005.08.048).

* Corresponding author. Tel.: +82 222603205; fax: +82 222603945.

E-mail addresses: absanj@yahoo.co.uk, abrarov@dongguk.edu (S.M. Abrarov).

sedimentation velocity up to 0.2–0.7 mm per hour for the balls ranging in diameter between 300 and 550 nm [10].

By means of the various chemical depositions, the voids of the opal matrix can be filled with semiconductors (GaAs, CdS, HgSe, Si, InN/GaN, CdTe, InP, ZnO, ZnS), superconductors (In, Pb) ferromagnetic materials (Fe and alloys) [11]. Different infiltration methods including chemical vapor deposition [12,13] chemical bath deposition [12], hydrolysis [13], salt-precipitation [13], sol-gel [13,14], electro-deposition [9,13], spray pyrolysis [13,15,16], etc. can be applied for the formation of nanoparticles in interglobular spaces of opal matrix.

Fig. 1 shows an experimental set for observation of Bragg reflection from the surface of opal matrix with perfectly assembled FCC structure. The reflection peak is detected according to Bragg's law

$$\lambda = 2d_{h,k,l}(n_{\text{eff}}^2 - \sin^2 \theta)^{1/2}, \quad (1)$$

where λ is the wavelength,

$$d_{h,k,l} = \frac{a}{\sqrt{h^2 + k^2 + l^2}},$$

a is the distance between planes, h , k , l are Miller indices, and n_{eff} is the effective refractive index. For opal with perfectly ordered balls, the experimental data excellently fit Bragg's law. Peak in reflectance (or dip in transmittance) shifts to the blue spectrum with increasing angle according to (1). However, an opal with imperfectly ordered silica balls behaves differently.

Consider Fig. 2 showing the SEM image of the opal, which FCC structure has dislocations, formed during the self-sedimentation process in a fluid suspension. The sample contains micro-size domains with facing up (111) and (100) planes. These domains are chaotically distributed within the sample and differently tilted with respect to its

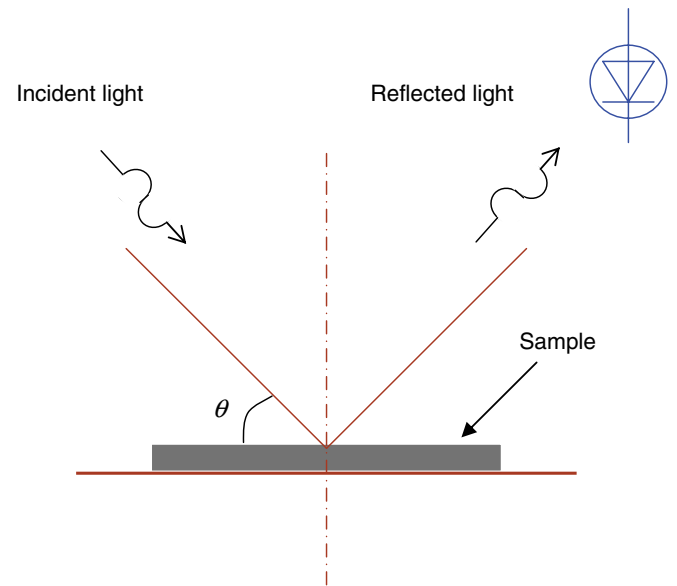


Fig. 1. Experimental set for observation of Bragg reflection in opal matrix with perfect FCC structure.

surface. As a result, the blue-shift in reflectance (or in transmittance) becomes insignificant and irregular with increasing angle [17,18]. It signifies that in highly imperfect or in amorphous opal the color remains practically stable at any θ (Fig. 1). Despite of the fact that such sample does not exhibit the blue-shift with increasing angle, the influence of photonic band-gap (PBG) in opal with disordered FCC structure is possible to observe conclusively either in the evolution of photoluminescence arising due to the gradual increase of the filling factor or in temperature-dependent photoluminescence [16].

It is worth remarking that imperfect opal structures exhibit spectrum with greater FWHM in reflection (or in

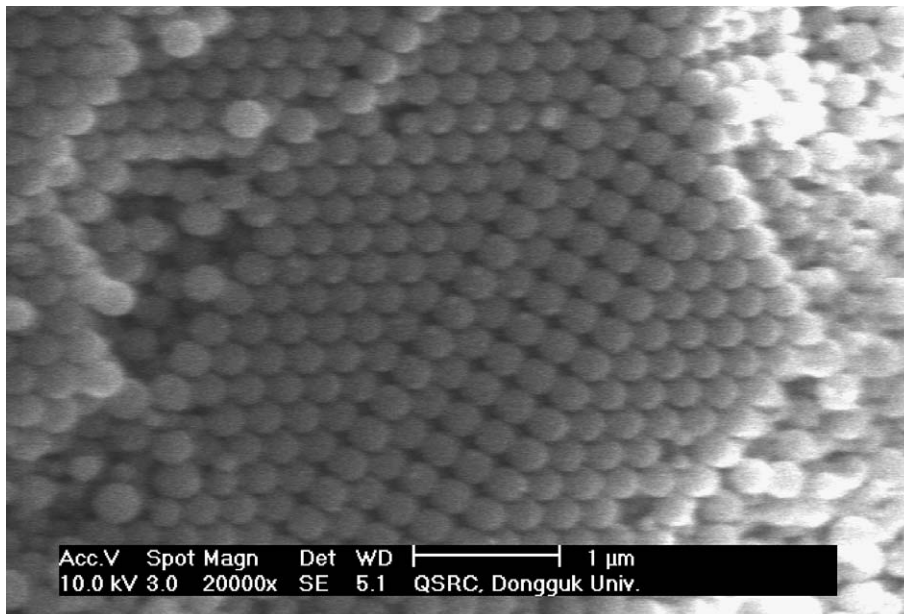


Fig. 2. SEM image of the opal comprising silica balls. The average diameter of spheres is 265 nm (orange opal).

transmission) [19]. While perfectly ordered opal matrix may find its applications in various light emitting devices [3,4], imperfectly assembled and/or amorphous opal with embedded luminescent nanoparticles might be useful for applications in full-color displays [16].

Nanoparticles infiltrated in interglobular spaces can considerably alter the optical properties of opal matrix. Therefore the estimation of the quantity of infiltrated nanocrystals plays a significant role in practice. Particularly, the amount of infiltrated material has to be properly controlled during its deposition in the voids.

This paper reports two filling factor equations based on effective medium and Maxwell–Garnett approximations. The comparison between them shows that both equations can be equally used for quantity estimation of infiltrated nanoparticles in interglobular spaces between FCC packed spheres.

2. Filling factor estimation

2.1. Refractive index based on effective medium approximation

The quantitative analysis of the optical characteristics of opal matrix can be significantly simplified introducing the effective refractive index according to effective medium approximation [20]. Effective refractive index can be defined as a weighted sum of indices of refraction n_1 , n_2 , n_3 , for spherical balls, infiltrated nanoparticles and air, respectively. For the bare and infiltrated opals, the effective refractive indices accordingly are

$$n_{\text{eff}_1} = n_1 \cdot 0.74 + n_3 \cdot 0.26 \quad (2a)$$

and

$$n_{\text{eff}_2} = n_1 \cdot 0.74 + n_2 \cdot f + n_3 \cdot (0.26 - f), \quad (2b)$$

where f is the filling factor for infiltrated nanocrystals. The values 0.74 and 0.26 are the filling factors for the host material (spherical balls) and air, respectively.

It is convenient to assume a low angle of incidence (Fig. 1). Substitution of definitions (2a) and (2b) into (1) yields wavelengths λ_1 , λ_2 for the bare and infiltrated opals. The refractive indices for the spherical balls and infiltrated nanoparticles are both, in general, wavelength dependent.

The red-shift in reflectance or transmittance spectra arising due to infiltrated nanocrystals inside opal matrix can be found as

$$\Delta\lambda = \lambda_2 - \lambda_1 = 2d_{h,k,l}(n_{\text{eff}_2} - n_{\text{eff}_1}). \quad (3)$$

Substituting definitions (2a) and (2b) into (3) yields the relation for the filling factor

$$f = \frac{\Delta\lambda}{2d_{h,k,l}} - (n_1(\lambda_2) - n_1(\lambda_1)) \cdot 0.74}{n_2(\lambda_2) - n_3}. \quad (4)$$

Alternatively, the filling factor can be derived through ratio between wavelengths λ_1 , λ_2 for the bare and infiltrated opals

$$\frac{\lambda_2}{\lambda_1} = \frac{2d_{h,k,l}n_{\text{eff}_2}}{2d_{h,k,l}n_{\text{eff}_1}}. \quad (5)$$

Substitution of effective refractive indices (2a) and (2b) into (5) results to

$$f = \frac{\frac{\lambda_2}{\lambda_1}(n_1(\lambda_1) \cdot 0.74 + n_3 \cdot 0.26) - (n_1(\lambda_2) \cdot 0.74 + n_3 \cdot 0.26)}{n_2(\lambda_2) - n_3}. \quad (6)$$

Clearly that (4) and (6) are equivalent. Substitution of expression $\lambda_1 = 2d_{h,k,l}n_{\text{eff}_1}$ into (6) leads to (4).

2.2. Effective refractive index based on Maxwell–Garnett approximation

Another definition for effective refractive indices, also widely used in practice, is based on Maxwell–Garnett approximation [21]. Effective refractive indices for the bare and infiltrated opals can be expressed as a weighted sum of the squared refractive indices

$$n_{\text{eff}_1}^2 = n_1^2 \cdot 0.74 + n_3^2 \cdot 0.26, \quad (7a)$$

$$n_{\text{eff}_2}^2 = n_1^2 \cdot 0.74 + n_2^2 \cdot f + n_3^2 \cdot (0.26 - f). \quad (7b)$$

Assume again a low angle of incidence. Substitution of definitions (7a) and (7b) into (1) provides two squared wavelengths λ_1^2 and λ_2^2 corresponding to the bare and infiltrated opals, respectively. The difference between them is

$$\lambda_2^2 - \lambda_1^2 = (2d_{h,k,l})^2(n_{\text{eff}_2}^2 - n_{\text{eff}_1}^2). \quad (8)$$

From (7a), (7b) and (8) the filling factor can be found as

$$f = \frac{\frac{\lambda_2^2 - \lambda_1^2}{(2d_{h,k,l})^2} - (n_1(\lambda_2)^2 - n_1(\lambda_1)^2) \cdot 0.74}{n_2(\lambda_2)^2 - n_3^2}. \quad (9)$$

Alternatively, the filling factor can be derived through following fraction:

$$\frac{\lambda_2^2}{\lambda_1^2} = \frac{4d_{h,k,l}^2 n_{\text{eff}_2}^2}{4d_{h,k,l}^2 n_{\text{eff}_1}^2}. \quad (10)$$

Substituting (7a) and (7b) into (10) leads to the relation for the filling factor

$$f = \frac{\frac{\lambda_2^2}{\lambda_1^2}(n_1(\lambda_1)^2 \cdot 0.74 + n_3^2 \cdot 0.26) - (n_1(\lambda_2)^2 \cdot 0.74 + n_3^2 \cdot 0.26)}{n_2(\lambda_2)^2 - n_3^2}. \quad (11)$$

Obviously (9) and (11) are equivalent. Substitution of expression $\lambda_1^2 = 4d_{h,k,l}^2 n_{\text{eff}_1}^2$ into (11) leads to (9).

Eqs (4), (6), (9) and (11) contain wavelength dependent terms $n_1(\lambda)$ and $n_2(\lambda)$. In order to represent them in analytic form, it is convenient to use Sellmeier dispersion formula providing excellent match for ZnO and SiO₂ [22–24]

$$n(\lambda)^2 = A + \frac{B\lambda^2}{\lambda^2 - C^2} + \frac{D\lambda^2}{\lambda^2 - E^2}, \quad (12)$$

where A , B , C , D and E are adjustable characteristics parameters.

3. Filling factors for opal matrix comprising silica balls

3.1. Refractive indices of silicon dioxide and zinc oxide

Fig. 3 shows the refractive indices for silicon dioxide and zinc oxide vs. wavelength. Analytical form of $n_1(\lambda)$ and $n_2(\lambda)$, obtained via Sellmeier dispersion approximation (12), quite accurately fit data available in literature [25,26]. The refractive index of ZnO may be considered a flat only at the wavelengths above 450 nm where in the most of the visible range it is around 2. Below this point, the refractive index of ZnO has strong wavelength dependence and its curve rapidly rises due to resonance occurring between valence and conduction bands.

Contrarily, the curve for the silicon dioxide is nearly flat. Therefore its refractive index can be considered a constant over the wide optical range covering near infrared (IR) to near ultraviolet (UV) spectra. Taking this into account and considering the fact that refractive index of air is very close to unity, (4) and (6) can be simplified and approximated as

$$f \approx \left\{ \begin{array}{l} \frac{\Delta\lambda}{2d_{h,k,l}(n_2(\lambda_2) - 1)}, \\ \frac{\Delta\lambda}{\lambda_1} \frac{n_1 0.74 + 0.26}{n_2(\lambda_2) - 1} \end{array} \right. \quad (13)$$

Similarly (9) and (11) can also be simplified and represented in form

$$f \approx \left\{ \begin{array}{l} \frac{\lambda_2^2 - \lambda_1^2}{4d_{h,k,l}^2(n_2(\lambda_2)^2 - 1)}, \\ \frac{\lambda_2^2 - \lambda_1^2}{\lambda_1^2} \frac{n_1^2 0.74 + 0.26}{n_2(\lambda_2)^2 - 1} \end{array} \right. \quad (14)$$

Suppose that the sample shown in Fig. 1 has the (111) plane facing up [27]. In this case

$$d_{1,1,1} = \frac{\sqrt{2}D}{\sqrt{3}} \approx 0.816D,$$

where D is the average spherical diameter. Substitution of the value $d_{1,1,1}$ into upper form of (13) results to

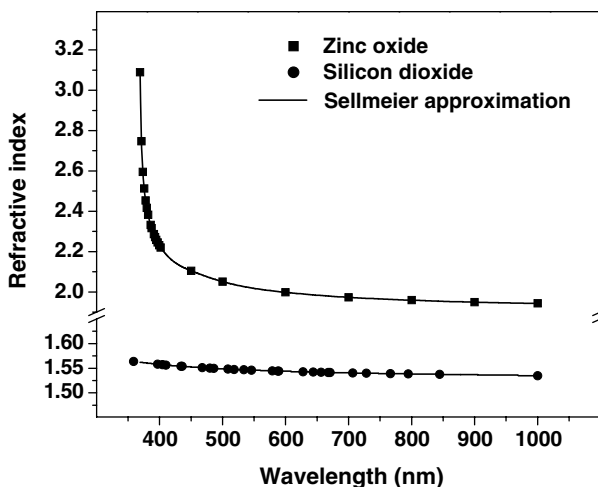


Fig. 3. Refractive indices for silicon dioxide and zinc oxide.

$$f \approx \frac{\Delta\lambda}{2D \times 0.816(n_2(\lambda_2) - 1)}. \quad (15)$$

Eq. (15) has been used for ZnO filling factor estimation in our previous work [28].

3.2. Discrepancies between filling factors

The relative error defined as

$$\text{err} = \frac{|f_1 - f_2|}{f_1} \times 100\% \quad (16)$$

is used in the present work to evaluate discrepancies between filling factors. Fig. 4 shows the filling factors and their relative errors (16) vs. red-shift. The filling factors f_1 and f_2 , calculated according to (13) and (14), are shown by solid and dashed curves, respectively.

Consider silica opals, which PBGs include near UV, visible (purple-blue, bluish-green, green, yellow, orange-red, crimson) and near IR spectra. Near origin the variations of the filling factors f_1, f_2 are comparatively high and their relative error strongly depends on diameter of silica balls. For UV opal with $D = 170$ nm the relative error is almost 10%, while for IR opal with $D = 310$ nm it is less than 4%. For all other opals with small infiltrations the relative errors are less than 8%.

Using the following relation $\lambda_2^2 - \lambda_1^2 = 2\Delta\lambda \times \lambda_1 + \Delta\lambda^2$ and (1), the Eq. (14) can be rearranged as

$$\frac{\lambda_2^2 - \lambda_1^2}{4d_{h,k,l}^2(n_2(\lambda_2)^2 - 1)} = \frac{\Delta\lambda}{d_{h,k,l}(n_2(\lambda_2)^2 - 1)} n_{\text{eff}1} + \frac{\Delta\lambda^2}{4d_{h,k,l}^2(n_2(\lambda_2)^2 - 1)}. \quad (17)$$

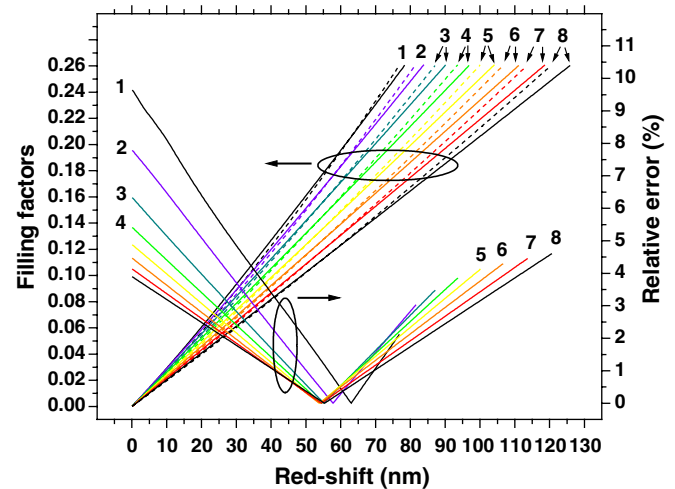


Fig. 4. Filling factors and relative error vs. red-shift for silica opals: 1—170 nm (near UV), 2—190 nm (purple-blue), 3—210 nm (bluish-green), 4—230 nm (green), 5—250 nm (yellow), 6—270 nm (orange-red), 7—290 nm (crimson), 8—310 nm (near IR). (For interpretation of the references in colour in this figure legend, the reader is referred to the web version of this article.)

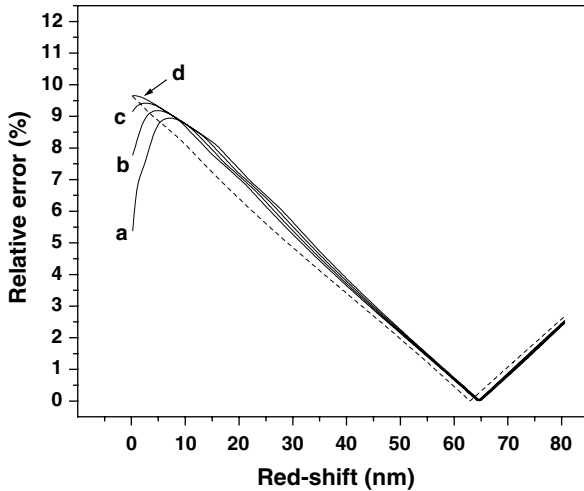


Fig. 5. Relative error vs. red-shift for UV opals.

At small infiltrations f_1 is greater than f_2 since the contributions from the second term on the right side of (17) is negligible due to the squared value $\Delta\lambda^2$ of the numerator. However, the second term gradually increases with increasing infiltration. The filling factors f_1, f_2 intercept each other in the red-shift range 55–65 nm indicating that the least discrepancies between them occur when $0.1 < f < 0.2$. At high infiltrations the contribution from the second term of (17) becomes significant leading to $f_1 < f_2$.

Fig. 5 shows relative error vs. red-shift dependencies for UV opals with average ball diameters: (a) 162, (b) 163, (c) 164, and (d) 165 nm. The dashed curve corresponding to $D = 170$ nm is also shown for comparison. From Fig. 5 one can see that the relative error does not further increase with decreasing average diameter of balls.

At the high infiltrations the relative errors are negligible for UV and purple-blue opals. For all other opals they do not exceed 5%. Discrepancies between filling factors show that each of two simplified Eqs. (13) and (14) can be used for the quantity estimation of infiltrated material inside silica opal. However, it should be taken into account that for the small amount of infiltration in UV opal the discrepancy may be relatively high, nearly 10%.

Even though the effective medium and Maxwell–Garnett approximations are successful to a certain extent to describe the optical properties of PhCs, both of them have the drawbacks, which may restrict the application range of (4) and (9). Presumably, the comparison between filling factors found via (4) and (9) and that of determined gravimetrically, i.e. by precise weighing of the samples before and after deposition [16,29], might be a helpful approach to demonstrate the practical limitations of the considered equations.

4. Filling factors for opal matrix comprising ZnO balls

In fact, both Eqs. (2a) and (7a) contain the term n_1 , which is itself, generally, may depend on value λ_1 . There-

fore when the refractive index of balls is a function of the wavelength, either of two Eqs. (2a) and (7a) contains two unknowns, namely λ_1 and $n_1(\lambda_1)$. This problem cannot be resolved analytically due to complicated form of Sellmeier dispersion formula (12). Iterating loop [30] is a useful and efficient programming method to solve numerically such a task. The basic objective in computation is to determine λ_1 and $n_1(\lambda_1)$, given by (2a) and (7a) via (12). Having known the exact values λ_1 and $n_1(\lambda_1)$, the filling factors $f_1(\Delta\lambda), f_2(\Delta\lambda)$ can be readily found through corresponding Eqs. (4) and (9), respectively.

The novel approach in fabrication of artificial opal comprising ZnO balls has been reported recently [19]. Refractive index of ZnO in the near UV spectrum is very high, exceeding 9 at the band edge [25,26]. Therefore, having such a high value of the refractive index, ZnO might be regarded a possible candidate in fabrication of opal matrix with complete PBG.

Gallium nitrate (GaN) can be synthesized inside the voids of opal matrix by means of chemical deposition, which details described elsewhere [31]. Suppose that GaN is infiltrated in ZnO opal. In such a combination n_1 and n_2 are refractive indices for ZnO balls and GaN, respectively. Unlike silica, ZnO is strongly wavelength dependent in the near UV region. Due to this reason, simplified Eqs. (13) and (14) cannot be applied for opal comprising ZnO balls when $\lambda_1 < 450$ nm.

The algorithm for computation of λ_1 and $n_1(\lambda_1)$ is straightforward. Consider λ_1 and $n_1(\lambda_1)$, related to effective medium approximation. Choose an arbitrary trial value of λ_1 , say 500 nm, and include it into Sellmeier dispersion formula (12). Find the corresponding refractive index of balls $n_1(\lambda_1)$ and substitute it into (2a). Calculate λ_1 by using (1) and compare it with previous value. If the difference between them is large, include the recent value λ_1 into Sellmeier dispersion formula and repeat all calculations again. Continue the same procedures if the difference between the recent and previous values of λ_1 is not greater than some small epsilon, say 10^{-3} nm.

The computation of λ_1 and $n_1(\lambda_1)$, related to Maxwell–Garnett approximation, is absolutely similar with the only difference that it employs (7a) instead of (2a). Typically the iteration consisting of just 20–40 calculation cycles (steps) is sufficient to get a required precision.

Table 1 shows the intermediate results for the opal with zinc oxide balls, which average diameter is supposed to be equal to 130 nm. The last row shows the exact values of λ_1 and $n_1(\lambda_1)$. The right part of Table 1 converges faster to the desired values due to squared form of (7a).

Fig. 6 shows filling factors and their relative error for ZnO opal infiltrated with GaN. The filling factors do not intercept. The curve for f_2 grows faster than that for f_1 , consequently the relative error monotonically increase. At the origin the relative error is small, less than 6%. However, at complete infiltration the discrepancy between filling factors becomes relatively high, reaching almost 16%.

Table 1
Intermediate results in iterative computation of λ_1 and $n_1(\lambda_1)$

Step	Effective medium approximation			Step	Maxwell-Garnett approximation		
	Trial λ_t , nm	Calculated λ_t , nm	$n_1(\lambda_t)$		Trial λ_t , nm	Calculated λ_t , nm	$n_1(\lambda_t)$
1	500.000	377.395	2.051	1	500.000	389.878	2.051
2	377.395	442.312	2.464	2	389.878	432.723	2.294
3	442.312	387.449	2.115	3	432.723	403.710	2.130
4	387.449	418.996	2.316	4	403.710	418.198	2.212
5	418.996	394.435	2.159	5	418.198	409.326	2.162
...
28	403.101	403.097	2.215	18	412.399	412.406	2.179
29	403.097	403.100	2.215	19	412.406	412.402	2.179
30	403.100	403.098	2.215	20	412.402	412.404	2.179
31	403.098	403.099	2.215	21	412.404	412.403	2.179
32	403.099	403.099	2.215	22	412.403	412.404	2.179

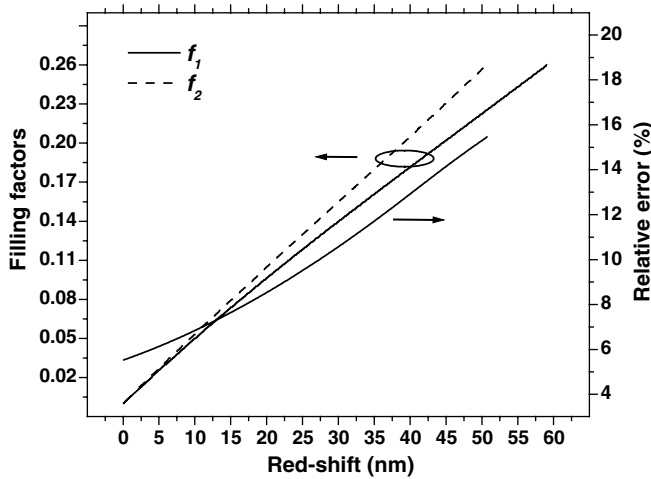


Fig. 6. Filling factors and relative error vs. red-shift for ZnO opal infiltrated with GaN.

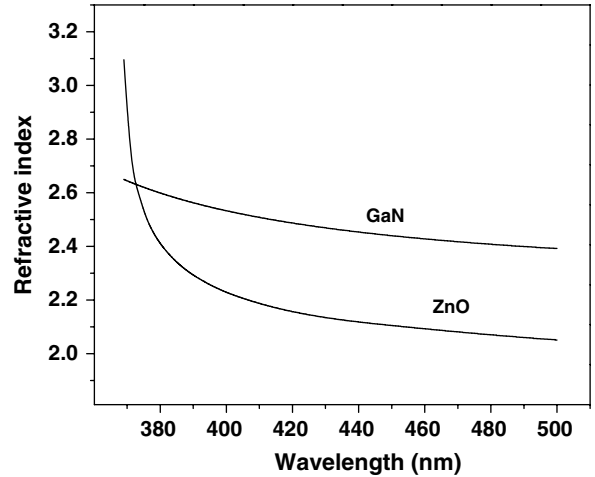


Fig. 7. Refractive indices of gallium nitride and zinc oxide.

Fig. 7 shows the refractive indices of GaN [24] and ZnO [25,26]. In the visible spectrum the refractive index of GaN is higher than that of ZnO. Analyzing (4) and (9) one can see that the relative error mostly depends on the diameter of the balls and the difference between refractive indices of the host and infiltrated materials. The decrease of the refractive index contrast increases the relative error between filling factors. For silica opal infiltrated with ZnO the difference between refractive indices is about 0.5 and more in the visible spectrum, while for ZnO opal infiltrated with GaN it is less than 0.35 (Fig. 7). As a result, the relative error for infiltrated ZnO opal is higher. It should be noted, however, that for the visible spectral range, the relative error between filling factors does not exceed 17.5% even at complete infiltration.

5. Conclusion

Two equations for the filling factor estimation of infiltrated ZnO in silica opal and GaN in ZnO opal have been considered. The first equation is based on effective medium approximation, while the second one—on Maxwell–Garnett approximation.

The filling factor equations can be simplified for the silica opal because of its weak dependence of refractive index on wavelength. However, the filling factor equations for opal comprising ZnO balls requires a numerical solution.

The comparison between filling factors shows that both of them can be equally used for quantity estimation of infiltrated material inside opal matrix. However, at complete infiltration the relative error between filling factors for

ZnO opal infiltrated with GaN may exceed 15% due to small refractive index contrast between zinc oxide balls and infiltrated gallium nitride nanoparticles.

Acknowledgements

This work is supported by the Korea Science and Engineering Foundation (KOSEF) through the Quantum-functional Semiconductor Research Center (QSRC), and by the research program and fund of Dongguk University, 2005.

References

- [1] E. Yablonovitch, *Phys. Rev. Lett.* 58 (1987) 2059.
- [2] S. John, *Phys. Rev. Lett.* 58 (1987) 2486.
- [3] J.J. Wierer, M.R. Krames, J.E. Epler, N.F. Gardner, M.G. Craford, J.R. Wendt, J.A. Simmons, M.M. Sigalas, *Appl. Phys. Lett.* 84 (2004) 3885.
- [4] M. Loncar, T. Yoshie, A. Scherer, P. Gogna, Y. Qiu, *Appl. Phys. Lett.* 81 (2002) 2680.
- [5] M. Koshihara, K. Saitoh, *Opt. Commun.* 253 (2005) 95.
- [6] A. Zakhidov, R. Baughman, Z. Iqbal, C. Cui, I. Khayrullin, S. Dantas, J. Marti, V. Ralchenko, *Science* 282 (1998) 897.
- [7] N.P. Johnson, D.W. McComb, A. Richel, B.M. Treble, R.M. De La Rue, *Synth. Metals* 116 (2001) 469.
- [8] W. Stöber, A. Fink, E. Bohn, *J. Colloid Interf. Sci.* 26 (1968) 62.
- [9] H. Yan, Y. Yang, Zh. Fu, B. Yang, L. Xia, Sh. Fu, F. Li, *Electrochem. Commun.* 7 (2005) 1117.
- [10] M. Trau, D.A. Saville, I.A. Aksay, *Science* 272 (1996) 706.
- [11] M.I. Samoilovich, S.M. Samoilovich, A.N. Guryanov, M. Yu. Tsvetkov, *Microelect. Eng.* 69 (2003) 237.
- [12] F. Meseguer, A. Blanco, H. Míguez, F. García-Santamaría, M. Ibisate, C. López, *Colloids Surf. A* 202 (2002) 281.
- [13] A. Stein, R.C. Schrodin, *Curr. Opin. Solid State Mater. Sci.* 5 (2001) 553.
- [14] R.M. Almeida, S. Portal, *Curr. Opin. Solid State Mater. Sci.* 7 (2003) 151.
- [15] S.M. Abrarov, Sh.U. Yuldashev, S.B. Lee, T.W. Kang, *J. Lumin.* 109 (2004) 25.
- [16] S.M. Abrarov, Sh.U. Yuldashev, T.W. Kim, H.Y. Kwon, T.W. Kang, *J. Lumin.* 114 (2005) 118.
- [17] D. Comoretto, R. Grassi, F. Marabelli, L.C. Andreani, *Mater. Sci. Eng. C* 23 (2003) 61.
- [18] A.S. Sinitskii, A.V. Knot'ko, Yu. D. Tretyakov, *Solid State Ionics* 172 (2004) 477.
- [19] E.W. Seelig, B. Tang, A. Yamilov, H. Cao, R.P.H. Chang, *Mater. Chem. Phys.* 80 (2003) 257.
- [20] W.L. Vos, R. Sprik, A. von Blaaderen, A. Imhof, A. La-gendijk, G.H. Wegdam, *Phys. Rev. B* 53 (1996) 16231; R.D. Pradhan, I.I. Tarhan, G.H. Watson, *Phys. Rev. B* 54 (1996) 13721.
- [21] J.C.M. Garnett, *Philos. Trans. R. Soc. London* 203 (1904) 385; J.C.M. Garnett, *Philos. Trans. R. Soc. London* 205 (1906) 237.
- [22] X.W. Sun, H.S. Kwok, *J. Appl. Phys.* 86 (1999) 408.
- [23] C.M. Herzinger, B. Johs, W.A. McGahan, J.A. Woollam, W. Paulson, *J. Appl. Phys.* 83 (1998) 3323.
- [24] G. Yu, G. Wang, H. Ishikawa, M. Umeno, T. Soga, T. Egawa, J. Watanabe, T. Jimbo, *Appl. Phys. Lett.* 70 (1997) 3209.
- [25] A.A. Blistanov, V.S. Bondarenko, N.V. Perelomova, F.N. Strizhevskaya, V.V. Chkalova, M.P. Shakof'skaya, *Acoustic crystals*, Moscow, Nauka, 1982, p. 216, 281.
- [26] Y.S. Park, J.R. Schneider, *J. Appl. Phys.* 39 (1968) 3049.
- [27] Due to crystal symmetry the sample can also be probed at the angle near to the surface normal. See, e.g., H. Míguez, C. López, F. Meseguer, A. Blanco, L. Vázquez, R. Mayoral, M. Ocaña, V. Fornés, A. Mifsud, *Appl. Phys. Lett.* 71 (1997) 1148.
- [28] S.M. Abrarov, Sh. U. Yuldashev, T.W. Kim, Y.H. Kwon, T.W. Kang, *Opt. Commun.* 259 (2006) 378.
- [29] S.A. Studenikin, N. Golego, M. Cocivera, *J. Appl. Phys.* 83 (1998) 2104.
- [30] H. Ruskeepää, *Mathematica Navigator*, Academic Press, New York, 1999, p. 451.
- [31] V. Yu. Davydov, R.E. Dunin-Borkovski, V.G. Golubev, J.L. Hutchison, N.F. Kartenko, D.A. Kurdyukov, A.B. Pevtsov, N.V. Sharenkova, J. Sloan, L.M. Sorokin, *Sem. Sci. Technol.* 16 (2000) L5.